Post-print version

A Simulation Analysis for Assessing the Reliability of AC/DC Hybrid Microgrids – Part II: Port Area and Residential Area

Antonio Bonì, Salvatore Favuzza, *Senior Member,* IEEE, Mariano Giuseppe Ippolito,
Fabio Massaro, Salar Moradi, Rossano Musca, Vincenzo Porgi, Gaetano Zizzo, *Senior Member,* IEEE
Engineering Department
University of Palermo
Palermo, Italy

***Abstract*—This paper reports the second part of a simulation study with the aim of evaluating the ability of two portions of a hybrid AC/DC MV/LV network in maintaining their operation in off-grid mode during the loss of the main AC grid due to a failure. In particular, this paper follows a dual purpose: first, it analysis two microgrids in a residential area and a port zone capability of operating in islanded mode, applying a probabilistic approach, while there is different energy use cases, and second is to evaluate some reliability indicators.**

***Keywords*—AC/DC microgrids; continuity; security; reliability; flexibility.**

I. INTRODUCTION

In the last decade, the scientific community has demonstrated an increase in researchers' interest in the concept of DC and hybrid AC/DC microgrids.

In [1], the authors present an exhaustive review of the power architectures, applications, and standardization issues for DC microgrids. In [2], the control strategies and stabilization techniques of such kinds of microgrids are analyzed. Also in [3], the authors face the problem of voltage control and energy management strategy of active distribution systems with a grid-connected DC microgrid as well as for an islanded DC microgrid with hybrid energy resources. In [4], an application of multilevel DC microgrids to residential buildings is presented, showing a method for optimizing the efficiency of DC/DC converters in parallel. In [5], a new and more flexible architecture for hybrid AC/DC microgrids with a multiport interlinking converter is proposed. Finally, in [6], a solar photovoltaic/battery energy storage-based microgrid with a multifunctional voltage source converter is presented. The above-cited papers represent only a small sample of the wide recent literature on the topic.

In particular, in this paper, the authors analyze the impact that different energy scenarios have on the hybrid network of a residential and a port area with charging stations for Electric Vehicles (EVs), in terms of the possibility of maintaining the continuity of supply for a given time. It is worth underlying that the study considers a very particular case: the microgrids are operating in islanded mode due to a fault took place at AC main supply, and are not equipped with specific devices for emergency power supply. What the study wants to investigate is, if it is possible and under which hypotheses, preserving a microgrid with specific features in operation during a fault with only its own local resources, increasing the reliability for its demand supply. A second challenge that the study tries to tackle is: how an increase in RES and ESS capacity can impact the results of such an analysis. Indeed, greater penetration of generating plants that exploit RESs, but also controllable loads, storage systems, and devices which are capable of implementing demand response actions are expected in the next decades.

In [6], the authors investigated experimentally the feasibility of a smooth transition from grid-connected to stand-alone mode of a microgrid using suitable control algorithms and presented a simple case with a storage system and a PV generator. The present study investigates the possibility of such a transition from an energy point of view. As the first step, five different energy scenarios are defined based on the last reports of Terna, WEC, REN21, ENTSO-E and other prominent organizations [7]-[11]. Then, four different microgrids are chosen and analyzed, showing the different behavior of each grid, dependent on the flexible resources and generators available: Photovoltaic (PV) and wind generators, controllable loads, static storage units and, EVs, and charging stations using V2G technology. Finally, some indicators defined by the same authors are calculated for assessing the reliability of each microgrid.

The four microgrids considered in this study are an underground station, a car parking with EV charging stations, a residential area downstream of a distribution substation, and a port area. In this paper, the residential and the port area microgrids are examined while the results of the study of the first two networks are presented in [12].

II. THE HYBRID AC/DC MICROGRIDS

Fig. 1 and Fig. 2 show the residential area and the port area microgrids, respectively. To study the behavior of both networks, in a preliminary phase, it is necessary to define the load and generation profiles that characterize them.

For the residential network, the presence of a 400 kVA MV/LV secondary substation has been hypothesized with a daily load diagram with a seasonal variation like that present in [13]. As regards the port network, it was assumed a consumption daily profile with no seasonal or monthly variations, linked to the services present within the port and defined by the study carried out in [14].

In both microgrids, there are distributed generation nodes with PV and wind power plants. By consulting the data base of the "Transparency Report" platform of the Italian TSO Terna [11], it was possible to examine an hour-based daily electricity produced data in Italy divided per primary source.

Therefore, the energy produced by wind and PV plants for the year 2020, and the daily data for each month of the year were collected. Each generic value $E_{i,j,k}$ of the database is a

This research was funded by the Research Fund for the Italian Electrical System under the Contract Agreement "Accordo di Programma 2019-2021 – PTR_19_21_ENEA_PRG_10" between ENEA and the Ministry of Economic Development. Progetto 2.7.

function of the i-th month, the j-th day, and the k-th hour, where:

- i = *January, February,…, December;*
- $j = 1, 2, \ldots, g_{max};$
- k = *00:00, 01:00, …, 24:00.*

with:

$$g_{max} = \begin{cases} 29, \text{ for Febrauary} \\ 30, \text{ for April, June, September, November} \\ 31, \text{ for the other month} \end{cases}$$

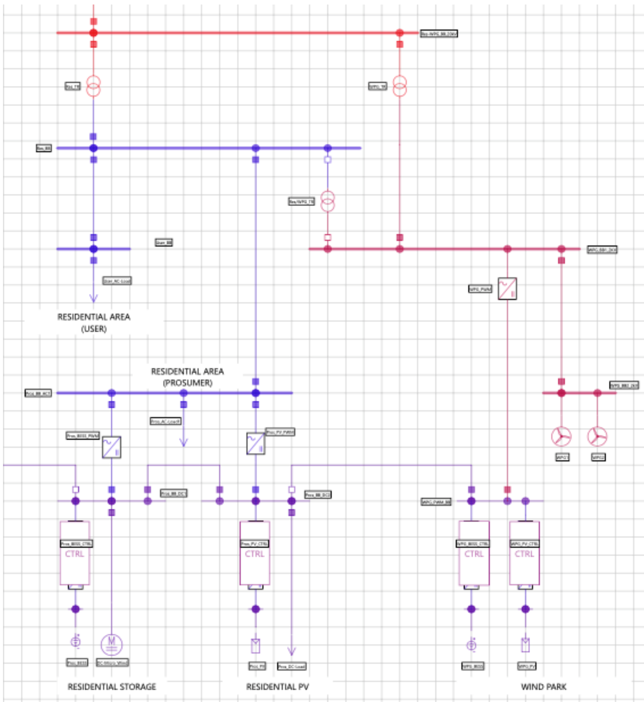

Fig. 1. Residential Area Network

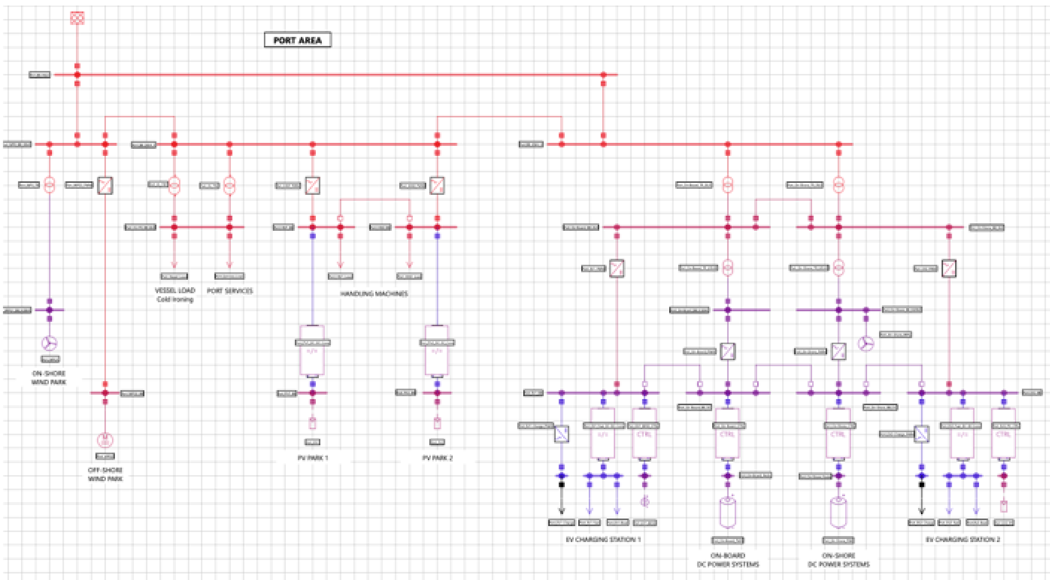

Fig. 2. Port Area Network.

The energy values $E_{i,j,k}$ refers to one hour, therefore it is possible to consider it as a equivalent single value for the average active power $P_{i,j,k}$ produced at the given hour. Fig. 3 and Fig. 4 show respectively the daily photovoltaic and wind generation profiles (in per unit) obtained.

Within the port area microgrid, there is a parking lot with slow- and fast-charging stations for EVs. For the first type of charging station a maximum power of 3 kW has been assumed. These stations are considered as the interruptible loads in the microgrid. For fast-charging stations, the maximum power of 10 kW is assumed and along with EVs are considered operating with V2G technology. The injection/consumption profiles of the EVs depend on the number of them connected to the network during the day and on the demand of the network [15].

As regards storage for the residential network and cold-ironing for the port network, the profiles vary according to the control logic applied and the microgrid load demand.

After extracting identified all power profiles in p.u., before proceeding with the simulations, it was necessary to identify, based on what was done in [12], the base values

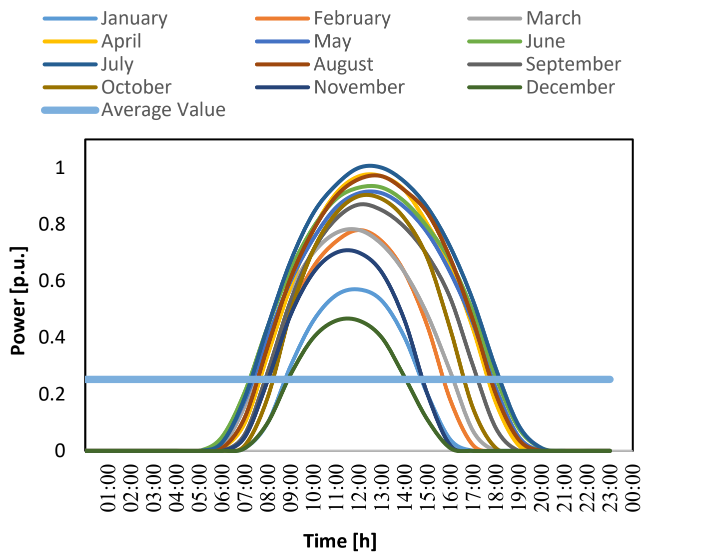

Fig. 3. Photovoltaic system power output expressed in [p.u.].

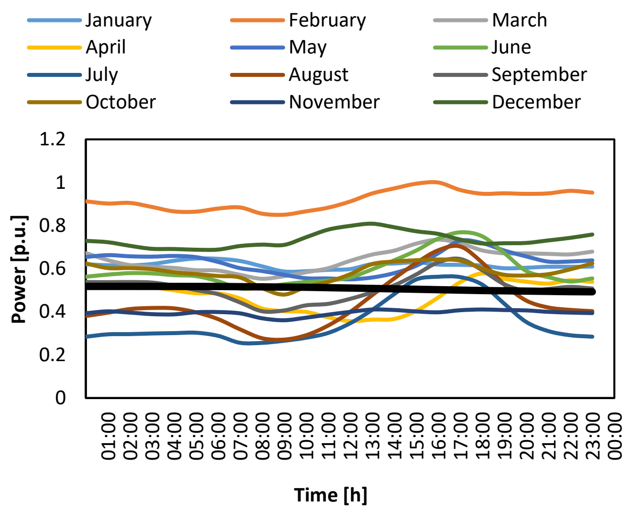

Fig. 4. Wind Farm power output expressed in [p.u.].

appropriately calculated for all the considered scenarios. In Table I, the base values deduced by [7]-[10] for the residential area microgrid for all scenarios are shown. In Table II, those related to the port area network are reported.

III. Calculation Code

The model is implemented in the MATLAB environment and is based on a probabilistic Montecarlo-type approach, simulates the island operation of the considered networks by randomly choosing the month, day, and instant at which the failure occurs. Having such information, it was possible to select the generation and consumption profiles relevant to the assessment. Therefore, the analysis of the above-described networks focuses on the time interval between the instant of failure extracted and the final instant, calculated as follows:

$$\textit{final time of the fault} = \textit{initial time of the fault} + \textit{duration of the fault}$$

where, the duration of the fault, according to [17], is assumed equal to 45 minutes for faults taking place in MV.

Depending on the time instant extracted, according to the profile in [16] concerning the percentage of EVs connected to the network during a typical day, it was possible to determine the number of fast-charging EVs and

TABLE I. Base Values for the Residential Network.

	2020	2030 BC	2030 DEC	2040 BC	2040DEC
Residential Consumption [kWh]	3696.00	3991.68	4213.44	4287.36	4656.96
Peak Value [kW]	280.00	302.40	319.20	324.80	352.80
PV Rated Power [kW]	33.00	43.00	60.00	62.00	87.00
Wind plants Rated Power [kW]	33.00	43.00	60.00	62.00	87.00
Storage Power [kW]	270	300	290	290	310
Energy Storage capacity [kWh]	540	600	580	580	620
n. EVs (Fast Charge) [-]	5	10	10	10	10
n. EVs (Slow charge) [-]	5	10	10	10	10

TABLE II. Base Values for the Port Network

	2020	2030 BC	2030 DEC	2040 BC	2040DEC
Port Consumption [kWh]	48559.11	52443.83	55357.38	56328.56	61184.47
Peak Value [kW]	4000.00	4320.00	4560.00	4640.00	5040.00
Controlled Load [kW]	200.00	216.00	228.00	232.00	252.00
PV Rated Power [kW]	320.00	570.00	1000.00	830.00	1470.00
Wind plants Rated Power [kW]	550.00	550.00	550.00	800.00	800.00
Cold Ironing Power [kW]	2000.00	2000.00	2000.00	4000.00	4000.00
Cold ironing Energy [kWh]	4000.00	4000.00	4000.00	8000.00	8000.00
n. EVs (Fast Charge) [-]	5	10	10	25	25
n. EVs (Slow charge) [-]	5	10	10	25	25

slow-charging EVs connected to the network through the charging columns. For each of them, through the Monte carlo extraction, the State of Charge (SoC) has been defined on which the charge/discharge time depends, considering that the EVs operate with SoC values between 10% and 90% of total capacity. Knowing the charging and discharging times for each EV, and comparing them with the duration of the failure, it was possible to determine the profile of the fast-charging EVs and the slow-charging EVs within the fault time range, considering that, depending on the network requirement, the former can operate in V2G, while the latter can operate as a flexible load to guarantee, where possible, island operation of the network and hence the balance between generated and absorbed active power. The same control logic was implemented with the storage present in the residential network and that of the ships connected with cold-ironing technology in the port network.

IV. RESULTS

The results obtained for all scenarios are shown below. According to the methodology explained in the first part of this study [12], various simulations were carried out for each scenario. Three of the most significant simulations (Simulations S1, S2, S3) are reported in the tables below. In particular, Table III indicates the capability of each microgrids to ensure operating in islanded mode during a 45-minute fault event: number 1 marks microgrids are able to operate in off-grid mode, and number 0 means they can not have a reliable operation during the fault event. Table IV, on the other hand, reports the minutes of the stand-alone operation for each simulation.

RES Index:

$$\dot{RES} = \frac{P_{RES}}{P_{load}} \cdot 100 \quad (1)$$

where:

- P_{RES}: total power generated by all the RES generation plants present in the considered microgrid;
- P_{LOAD}: total load of the microgrid;

1) FLEX Index:

$$FLEX = \frac{P_{load,flex}}{P_{load}} \cdot 100 \quad (2)$$

where:

TABLE III. ISLANDING MODE INDEX

	RESIDENTIAL AREA NETWORK			PORT AREA NETWORK		
	S1	S2	S3	S1	S2	S3
2020	0	0	1	0	1	0
2030-BC	1	0	0	0	1	0
2030-DEC	0	0	1	0	0	0
2040-BC	0	0	0	0	0	0
2040-DEC	0	0	1	0	0	1

TABLE IV. RANGE TIME IN ISLANDING MODE

	RESIDENTIAL AREA NETWORK			PORT AREA NETWORK		
	S1	S2	S3	S1	S2	S3
2020	00:40	00:33	00:45	00:00	00:45	00:00
2030-BC	00:45	00:15	00:36	00:00	00:45	00:00
2030-DEC	00:21	00:09	00:45	00:00	00:00	00:00
2040-BC	00:25	00:38	00:16	00:00	00:00	00:27
2040-DEC	00:16	00:32	00:45	00:19	00:27	00:45

- $P_{load,FLEX}$ the total power of flexible loads of the microgrids;

2) BESS Index:

$$\dot{BESS} = \frac{P_{BESS}}{P_{load}} \cdot 100 \quad (3)$$

where:

- P_{BESS} the total power supplied/consumed by all storage systems;

3) i_1 Index:

$$i_1 = \frac{h_i}{T} \cdot 100 \quad (4)$$

where:

- h_i: the time duration at which given microgrid can operatein islanded mode;
- T: failure duration;

4) i_2 Index:

$$i_2 = \frac{\Delta P_{load.flex} + \Delta P_{RES} + \Delta P_{BESS}}{A_n} \cdot 100 \quad (5)$$

where:

- A_n is the apparent power of the node to which the portion of the considered network is connected;
- ΔP_{RES} is the average variation, in the time interval of the failure, of the total power generated by all RES generation plants present in the microgrid;
- $\Delta P_{load.flex}$ is the average variation, in the time interval of the failure, of the total power of the flexible loads;
- ΔP_{BESS} is the average variation, in the time interval of the fault, of the total power delivered by the storage
- systems in the microgrid, required by the AC network.

5) i_3 Index:

$$i_3 = \frac{\Delta E_{flex(T)}}{E_{th}} \cdot 100 \quad (6)$$

where:

- $\Delta E_{flexe(T)}$: energy supplied by the flexible devices present in the microgrid in the time interval of the fault;
- E_{th} : energy required to ensure island operation of the portion of the considered network in the time interval of the fault.

For each simulation and for each microgrid (residential and port area), the indicators are reported at Tables from V to XVI.

A. Residential Area Network

TABLE V. *RES* INDEX

Scenario	*Simulation 1*	*Simulation 2*	*Simulation 3*
2020	20%	35%	9%
2030 BC	10%	44%	16%
2030 DEC	33%	46%	9%
2040 BC	42%	52%	15%
2040 DEC	53%	61%	20%

TABLE VI. *FLEX* INDEX

Scenario	*Simulation 1*	*Simulation 2*	*Simulation 3*
2020	20%	33%	0%
2030 BC	0%	43%	43%
2030 DEC	33%	40%	0%
2040 BC	27%	12%	42%
2040 DEC	23%	12%	42%

TABLE VII. *BESS* INDEX

Scenario	*Simulation 1*	*Simulation 2*	*Simulation 3*
2020	60%	32%	91%
2030 BC	90%	14%	62%
2030 DEC	34%	14%	91%
2040 BC	31%	36%	43%
2040 DEC	24%	29%	80%

TABLE VIII. i_1 INDEX

Scenario	Simulation 1	Simulation 2	Simulation 3
2020	67%	33%	100%
2030 BC	100%	0%	33%
2030 DEC	33%	0%	100%
2040 BC	33%	67%	33%
2040 DEC	33%	67%	100%

TABLE IX. i_2 INDEX

Scenario	Simulation 1	Simulation 2	Simulation 3
2020	24%	31%	37%
2030 BC	32%	37%	59%
2030 DEC	24%	39%	68%
2040 BC	35%	41%	62%
2040 DEC	25%	45%	56%

TABLE X. i_3 INDEX

Scenario	Simulation 1	Simulation 2	Simulation 3
2020	76%	49%	100%
2030 BC	100%	24%	58%
2030 DEC	51%	26%	100%
2040 BC	53%	74%	53%
2040 DEC	53%	72%	100%

B. Port Area Network

TABLE XI. *RES* INDEX

Scenario	Simulation 1	Simulation 2	Simulation 3
2020	12%	36%	13%
2030 BC	22%	18%	27%
2030 DEC	29%	11%	25%
2040 BC	34%	44%	29%
2040 DEC	13%	57%	35%

TABLE XII. *FLEX* INDEX

Scenario	Simulation 1	Simulation 2	Simulation 3
2020	7%	22%	5%
2030 BC	6%	26%	7%
2030 DEC	20%	6%	5%
2040 BC	7%	29%	7%
2040 DEC	19%	9%	19%

TABLE XIII. *BESS* INDEX

Scenario	Simulation 1	Simulation 2	Simulation 3
2020	35%	42%	13%
2030 BC	30%	55%	65%
2030 DEC	8%	57%	45%
2040 BC	1%	22%	28%
2040 DEC	20%	13%	46%

TABLE XIV. i_1 INDEX

Scenario	Simulation 1	Simulation 2	Simulation 3
2020	0%	100%	0%
2030 BC	0%	67%	0%
2030 DEC	0%	0%	0%
2040 BC	0%	33%	33%
2040 DEC	33%	67%	100%

TABLE XV. i_2 INDEX

Scenario	Simulation 1	Simulation 2	Simulation 3
2020	6%	4%	5%
2030 BC	8%	4%	12%
2030 DEC	3%	11%	13%
2040 BC	6%	4%	9%
2040 DEC	4%	9%	6%

TABLE XVI. i_3 INDEX

Scenario	Simulation 1	Simulation 2	Simulation 3
2020	47%	100%	20%
2030 BC	52%	100%	98%
2030 DEC	43%	72%	68%
2040 BC	12%	91%	55%
2040 DEC	43%	59%	100%

Analyzing the data in Table III, it is possible to assert that: in 26.67% of the simulations carried out for the residential area network it is possible to keep islanded mode; and in 20% of the simulations carried out for the port network it is possible to keep islanded mode.

These low percentage values are justified by the fact that there are services/activities that have a daily load profile that changes with sudden variations over time and therefore difficult to feed through generation from RES and/or storage systems.

The contributions of RES, storage and flexible loads in the different energy scenarios from 2020 to 2040, on the other hand, seem to have an insignificant influence on the outcome of the simulations.

It is of particular interest to analyze the data in Table IV where, for all simulations, the time for which the network is able to maintain islanding is shown. Note is that, while the residential network is almost able to operate in off-grid mode even for a few minutes, in the simulations of the port network there is a clear cut so that the network is capable of preserving islanded mode for low number of simulations in the fault duration (only 20% of the simulations). This consideration is found to a lesser extent in the 2040-BC and 2040-DEC scenarios, where the growing size of storage, cold ironing and V2G EVs allow for greater load coverage. The result above is obviously reflected in the calculation of the indicators.

Also for these two microgrids, like for those examined in [12], the i_1 index shows its variability as a function of the instant in which the fault occurs, the availability of charge in the batteries, and, in general, of the resources of the network. The residential area microgrid shows higher values of this indicator for almost all simulations. This is due to the lower load. The same can't be said for the underground station.

i_2 is, in general, lower in the port area (from 3% to 13%) than in the residential area (from 24% to 68%) and this indicates that in realistic scenarios like those considered in this work, for the port area microgrid, the power variation at the point of common coupling is, in general, not significant.

Finally, i_3 is always high, showing that the considered microgrids can contribute to the main grid needs by modifying their consumption and increasing the grid reliability.

Finally, it is important to underline that in order for DC microgrids to be effectively able to improve the reliability of a distribution system, a technological leap is necessary regarding the introduction in networks such as reliable supervision and control systems, reclosure systems rapid backup lines, electronic DC / DC and DC / AC converters which are capable of being totally enslaved by the island's Energy Management System in order to guarantee the operation of the network.

All of this is still under study and is a central theme of research on Smart Grids and the Electrical System.

V. Conclusion

The present work has been carried out in the framework of the project “2.7 Modelli e strumenti per incrementare l'efficienza energetica nel ciclo di produzione, trasporto, distribuzione dell'elettricità”, PTR 2019-2021. The paper has presented a simulation analysis of the reliability of two microgrids, investigating how the presence of flexible resources and local generators can increase the possibility of operating in stand-alone mode in case of loss of the main grid. Two sets of indicators have been calculated: the first one for characterizing the microgrids with regards to the presence of storage system, flexible load, and RES generators, the second one for assessing the microgrids reliability. In general, it can be concluded that, in realistic scenarios based on the elaboration of the most recent projections of prominent energy and electrical organization, distributed flexible resources seems not be able to support solely the operation of hybrid microgrids for more than 15-30 minutes (as an average), that is less than the average failure recovery time for Italian networks.

References

[1] T. Dragicevic, X. Lu, J. C. Vasquez, J. M. Guerrero, “DC microgrids—part I: a review of power architectures, applications, and standardization issues”, IEEE Transactions on Power Electronics, Vol. 31, No. 5, 2016, pp. 3528-3549.

[2] T. Dragicevic, X. Lu, J. C. Vasquez, J. M. Guerrero, “DC microgrids—part I: a review of control strategies and stabilization techniques”, IEEE Transactions on Power Electronics, Vol. 31, No. 7, 2016, pp. 4876-4891.

[3] S. Pannala, N. Patari, A. K. Srivastava, N. P. Padhy, “Effective control and management scheme for isolated and grid connected DC microgrid”, IEEE Transactions on Industry Applications, Vol. 56, No. 6, pp. 6767-6780.

[4] V. Boscaino, J. M. Guerrero, I. Ciornei, L. Meng, E. Riva Sanseverino, G. Zizzo, “Online optimization of a multi-conversion-level DC home microgrid for system efficiency enhancement”, Sustainable Cities and Society, Vol. 35, 2017, pp. 417-429.

[5] J. Khodabakhsh, G. Moschopoulos, “Simplified hybrid AC–DC microgrid with a novel interlinking converter”, IEEE Transactions on Industry Applications, Vol. 56, No. 5, 2020, pp. 5023-5034.

[6] V. Narayanan, S.a Kewat, B. Singh, “Solar PV-BES based microgrid system with multifunctional VSC”, IEEE Transactions on Industry Applications, Vol. 56, No. 3, 2020, pp. 2957-2967

[7] REN 21, «Renewables 2019 global status report,» REN 21, 2019.

[8] World Energy Council, “Energy storage monitor, latest trends on energy storage”, WEC, 2019.

[9] Terna SpA, SNAM, “Documento di descrizione degli scenari 2019”, 2019.

[10] ENTSO-E, ENTSOG, “TYNDP 2020, scenario report”, 2020.

[11] Terna SpA, “Transaparency report”, available at: https://www.terna.it/it/sistema-elettrico/transparency-report/actual-generation.

[12] A. Bonì, S. Favuzza, F. Massaro, R. Musca, V. Porgi, G. Zizzo, “Analysis of scenarios for assessing the reliability of AC/DC hybrid microgrids – part I: underground station and car parking”, IEEE EEEIC/I&CPS Europe 2021, 7-10 October 2021, Bari (Italy).

[13] RSE, “Analisi di impatto dell’introduzione della tariffa bioraria obbligatoria”, Technical Report 13000580, 2012.

[14] G. Parise, L. Parise, L. Martirano, P. B. Chavdarian, Chun-Lien Su, A. Ferrante, “Wise port and business energy management: port facilities, electrical power distribution”, IEEE Transactions on Industry Applications, 2015, 52.1: 18-24.

[15] L. Lin, X. Liu, T. Zhang, X. Liu, “Energy consumption index and evaluation method of public traffic buildings in China”, Sustainable Cities and Society, Vol. 57, 202 , article 102132.

[16] J. A. Peças Lopes, F. J. Soares, P. M. Almeida, M. Moreira da Silva, “Smart charging strategies for electric vehicles: enhancing grid performance and maximizing the use of variable renewable energy resources”, EVS24, 13-16 May 2009, Stavanger (Norway).

[17] ARERA, “Dati sulla continuità del servizio elettrico”, https://www.arera.it/sas-frontend-cse/estrattoreLink”.